MISCIBILITY OF POLYMERS COMPRISING WOOD CELL WALL

重松, 幹二
九州大学農学研究科林産学専攻

https://doi.org/10.11501/3086537

出版情報：九州大学, 1991, 博士（農学）, 課程博士
バージョン：
権利関係：

Chapter 3

Vapor Pressure Osmometry Studies on Solution Properties of Hemicellulose, Lignin and Their Mixture

3.1 Introduction

In Chapter 1 and 2, the adhesion and miscibility between polysaccharides and lignin were described. Particularly, Flory polymer-polymer interaction parameter between hemicellulose and lignin (χ_{12}) was observed in Chapter 2. This result shows the χ_{12} is positive and decreases with lignin content and temperature. The temperature dependence, however, is determined at above 140 ˚C, because the miscibility was not observed below it. This chapter deals to solution properties of hemicellulose and lignin in dimethylsulphoxide (DMSO) in the temperature range of 60 - 90 ˚C. Moreover, the temperature dependence of χ_{12} in this temperature region was evaluated.

There are several methods for measurement of χ_{12}, such as osmotic pressure [77] or small-angle neutron scattering [78]. In this research, the solution properties of solutions of woody polymer were investigated by a vapor pressure osmometric (VPO) measurement. First, activities were measured for polymer-solvent solutions, from which we derived the interaction between polymer and solvent. Secondly, activities were measured for polymer-polymer-solvent solutions and thus we were able to obtain the excess interaction of the ternary solution over the binary solution. This excess interaction corresponds to the interaction between polymer and

polymer and is quantitatively expressed by Flory polymer-polymer interaction parameter, χ_{12}.

There are many solvent for lignin, *e.g.*, pyridine, DMF, DMSO and dioxane etc. [79]. However, hemicellulose have a little solvent, *e.g.*, NaOH aq. and DMSO. Hence, if we want to know the interaction between these polymers by VPO in solutions, only DMSO is useful for measurement.

3.2 Experimental

3.2.1 *Materials*

Hemicellulose and lignin were prepared from wood meal of beech (*Fagus crenata* Bl.) in the same manner as described previously (Section 1.2.1).

Dimethylsulfoxide (DMSO) used as a solvent was purchased from Wako Pure Chemical Industries, Ltd. (Japan) and used without further purification. Solutions were mixed and stored at room temperature for one week.

3.2.2 *Molecular weight*

The number average molecular weight ($\overline{M}_n$) was evaluated in DMSO at 60 ˚C by using a vapor pressure osmometer (VPO) made by Knauer Co., Ltd. (Germany). The concentration range was 0.1 - 0.5 g/g. $\overline{M}_n$ is obtained by plotting $\Delta R/C$ vs. C and dividing K_1 by the ordinate intercept; ΔR (Ω) is the resistance difference of the two thermistors placed in the drops of solution and solvent, K_1 (g/mol·Ω) is the calibration constant determined by using benzil (M.W.=240) as a standard, and C (g/g) is the concentration of solution.

The viscosity average molecular weight ($\overline{M}_v$) for hemicellulose and lignin were calculated from the intrinsic viscosity in DMSO and in pyridine at 25 ˚C, respectively. The viscosity-molecular weight relationship used are

$$[\eta] = 5.9\times10^{-3}\overline{DP}_w^{0.94} = 0.65\overline{M}_w^{0.94} \quad \text{for hemicellulose [37],}$$

$$[\eta] = 0.0135\overline{M}_w^{0.175} \quad \text{for lignin [38],}$$

where $[\eta]$ (dl/g) is intrinsic viscosity, $\overline{DP}_w$ is degree of polymerization based on the weight-average molecular weight, $\overline{M}_w$.

3.2.3 *Measurement of Activity*

The activity of solvent (a_o) in solution was evaluated from $\ln a_o = - \Delta R/K_2$ by using a VPO, where K_2 (mol/mol·Ω) is the calibration constant determined in the same manner as K_1. Values of a_o were measured at 60 - 90 °C and 0.1 - 0.5 g/g.

3.3 Results and Discussion

3.3.1 *Thermodynamic parameters of dilution*

The free energy of dilution ($\Delta\bar{G}_o$) is calculated from the activity of solvent in solution (a_o) by

$$\Delta\bar{G}_o = RT \ln a_o, \qquad (3\text{-}1)$$

where R is the gas constant and T is the absolute temperature.

The variation of $\Delta\bar{G}_o$ with concentration at 60 ˚C for hemicellulose and lignin is shown in Fig. 3-1. The viscosity of the hemicellulose solution was high, and a concentration of 0.3 g/g was an upper limit for measurement. The large negative values of $\Delta\bar{G}_o$ indicate that at 60 ˚C the DMSO is a good solvent for both hemicellulose and lignin.

Figure 3-2 shows the dependence of $\Delta\bar{G}_o$ on temperature at constant concentration in 0.3 g/g. Since the decomposition of DMSO took place above 100 ˚C, the measurements were limitted below 90 ˚C. DMSO is a better solvent for lignin between 60 ˚C and 90 ˚C, because absolute values of $\Delta\bar{G}_o$ are lower for lignin than for hemicellulose. For both polymers, $\Delta\bar{G}_o$ increased with an increase in temperature. Thus DMSO seems to become a "*poorer solvent*" for polymers with an increase in temperature. This tendency was more distinct for lignin, because the elevation of $\Delta\bar{G}_o$ was higher for lignin than for hemicellulose.

The enthalpy ($\Delta\bar{H}_o$) and the entropy ($\Delta\bar{S}_o$) of dilution are obtained from

$$\Delta\bar{H}_o = \delta(\Delta\bar{G}_o/T)/\delta(1/T), \qquad (3\text{-}2)$$

$$-T\Delta\bar{S}_o = T\delta\Delta\bar{G}_o/\delta T \quad \text{or} \quad = \Delta\bar{G}_o - \Delta\bar{H}_o, \qquad (3\text{-}3)$$

by substitution of the value of $\Delta\bar{G}_o$ at various temperatures. Figure 3-3 shows the plot of $\Delta\bar{G}_o/T$ vs. $1/T$. The enthalpy was estimated to be -76 J/mol for hemicellulose and -420 J/mol for lignin. The negative value of $\Delta\bar{H}_o$ corresponds to exothermic dilution, which indicates that the solute-solvent interaction exceed solute-solute and solvent-solvent interactions.

Values of $\Delta\bar{S}_o$ from Eq. 3-3 were low, being -0.092 J/mol·K for hemicellulose and -0.855 J/mol·K for lignin. The negative value of $\Delta\bar{S}_o$ indicates a small decrease in randomness between solute and solvent molecules. This is probably caused by the strong interaction between solvent and solute as shown by the substantial changes in $\Delta\bar{H}_o$.

Brown [80] has obtained the thermodynamic parameters of the solution of kraft lignin in various solvents, *e.g.*, DMSO, dimethylformamide and 1,4-dioxane. It was found that DMSO was the "best solvent" since it gave the largest negative value of $\Delta\bar{G}_o$ (and, as discussed later, the smallest value of χ_{o2}). The values of $\Delta\bar{G}_o$, $\Delta\bar{H}_o$, and $\Delta\bar{S}_o$ measured by Brown were -105 J/mol, 71.6 J/mol and 177 J/mol·K, respectively, at 52 ° C and a concentration of 0.3 g/g in DMSO. Brown's value of $\Delta\bar{G}_o$ and mine are consistent with each other; however, the results of $\Delta\bar{H}_o$ and $\Delta\bar{S}_o$ differ considerably. This may be caused by differences in the method of preparation of the lignin, and/or differences in the moisture content; present samples were absolutely dry while his contained 2% moisture.

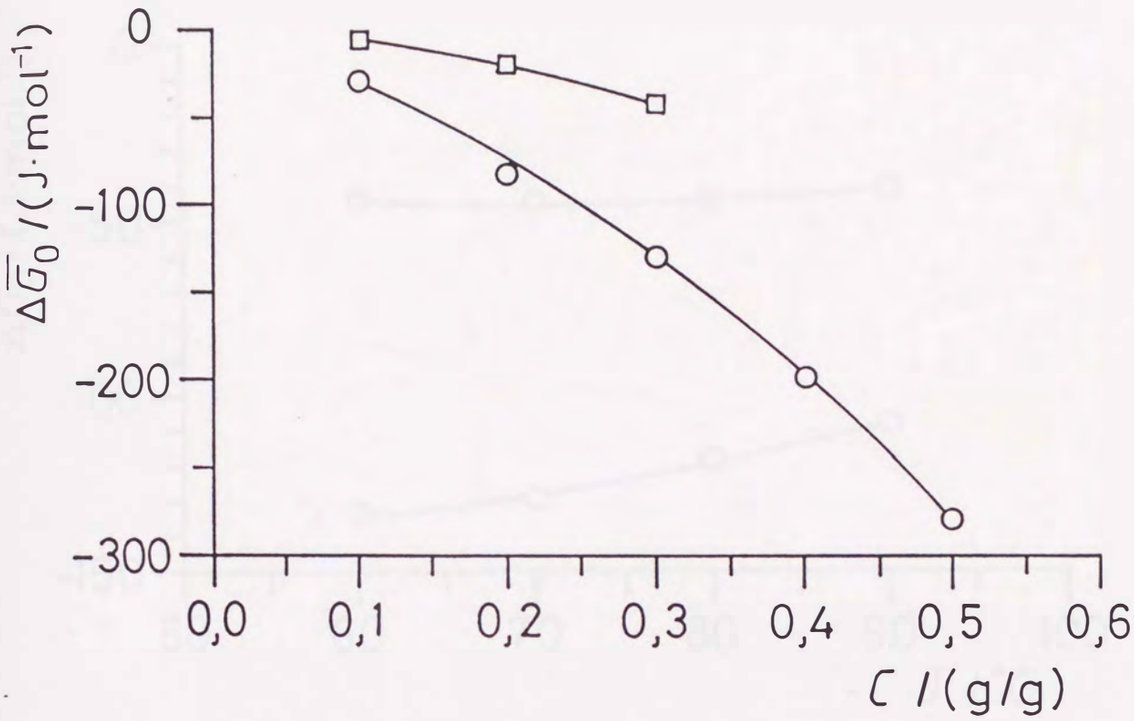

Fig. 3-1 Concentration dependence of the free energies of dilution ($\Delta\bar{G}_o$) for hemicellulose-DMSO (□) and lignin-DMSO (○) solutions observed by a vapor pressure osmometer. Temperature is constant at 60 ° C.

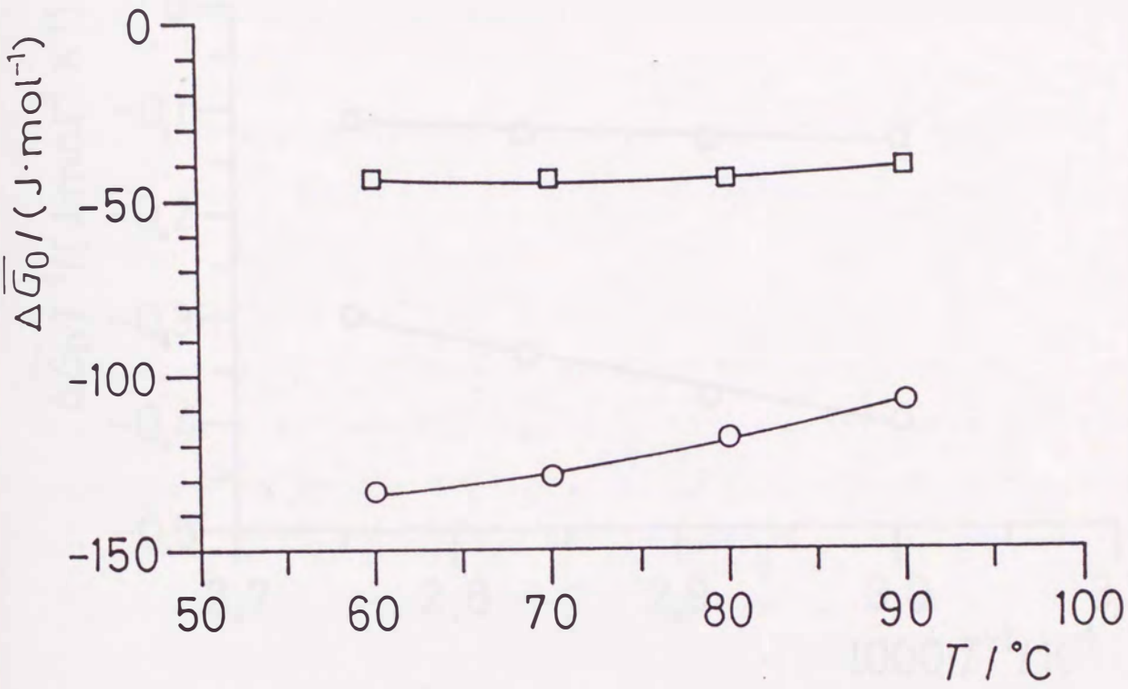

Fig. 3-2 Temperature dependence of the free energies of dilution ($\Delta\bar{G}_o$) for hemicellulose-DMSO (□) and lignin-DMSO (○) solutions. Concentration is constant of 0.3 g/g.

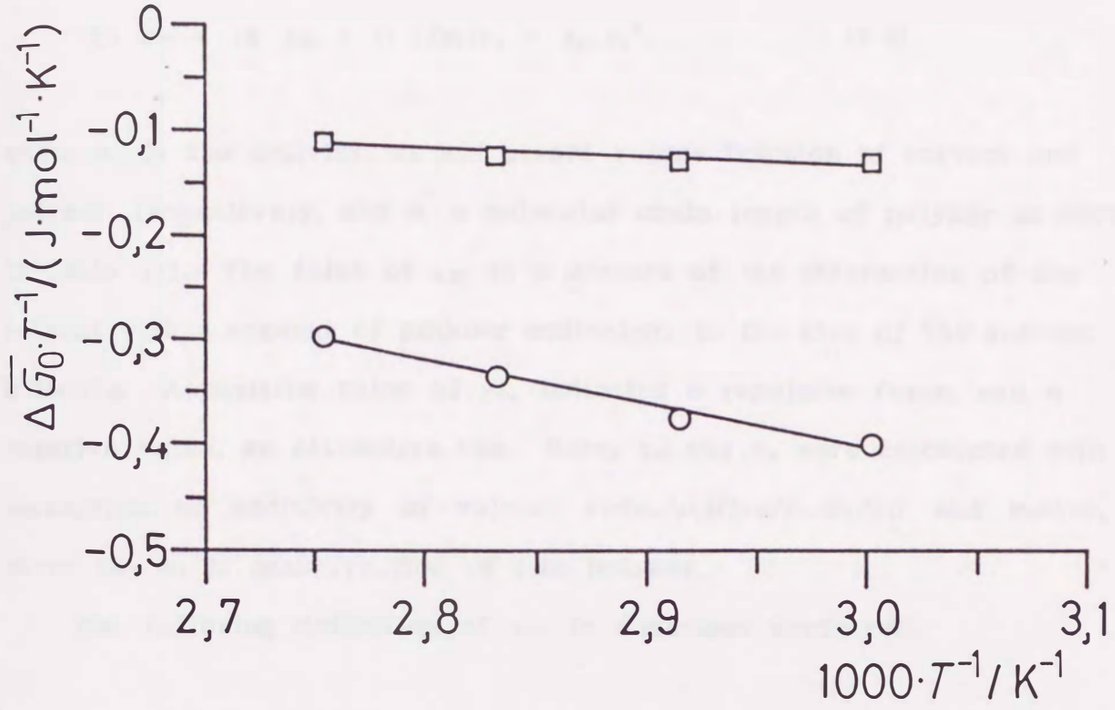

Fig. 3-3 Plots of $\Delta\bar{G}_o/T$ vs. $1/T$ of hemicellulose-DMSO (□) and lignin-DMSO (○) solutions at 0.3 g/g. Slope denotes the enthalpy of dilution ($\Delta\bar{H}_o$).

3.3.2 *Interaction parameters between solvent and solute*

The Flory interaction parameter between solvent and solute segments (χ_{oi}) is obtained from Eq. 3-4 [24],

$$-\ln a_o = \ln v_o + (1-1/m_i)v_i + \chi_{oi}v_i^2, \qquad (3\text{-}4)$$

where a_o is the activity, v_o and v_i are volume fraction of solvent and polymer, respectively, and m_i a molecular chain length of polymer as shown in Table 1-1. The value of χ_{oi} is a measure of the interaction of the solvent with a segment of polymer equivalent to the size of the solvent molecule. A positive value of χ_{oi} indicates a repulsive force, and a negative value, an attractive one. Here, v_o and v_i were calculated with the assumption of additivity of volume; $v_i=(w_i/\rho_i)/(w_o/\rho_o+w_i/\rho_i)$ and $v_o=1-v_i$ where the w_i is mass fraction of i-th polymer.

The following definition of χ_{oi} is sometimes preferred,

$$\chi_{oi} = \Lambda V_o/RT, \qquad (3\text{-}5)$$

where Λ is constant and represents the interaction energy density characteristic of the solvent-solute pair. If the constant Λ is essentially independent of concentration and temperature, χ_{oi} is proportional to $1/T$ and independent of concentration.

According to the theory of Flory and Huggins, equation 3-4 is valid for linear polymers. There is no equivalent theory for branched polymers. The hemicellulose is slightly branched. Lignin is believed to be branched and to have a three-dimensional structure [36]. Therefore application of the Flory-Huggins theory to present system will not be rigorously correct.

However the errors involved for the low-molecular-weights substances in the present works can be expected to be small. Also we are considering the variation of χ_{o1} with temperature rather than absolute values of χ_{o1}. Thus the use of the theory for linear molecules is justified.

The values of χ_{o1} for various lignin and hemicellulose concentrations are shown in Fig. 3-4. Both χ_{o1} and χ_{o2} increased with an increase of concentration and approached to the value of 0.5 which is limit of theoretical value and corresponds to the occurrence of phase separation. The trend for lignin is consistent with the data published by Brown [80].

As shown in Fig. 3-5, both χ_{o1} and χ_{o2} increased with an increase in temperature and were proportional to $1/T$. It is apparent that DMSO becomes a "poorer solvent" for both hemicellulose and lignin with an increase in temperature. This result is consistent with data for the thermodynamic parameters of dilution in the previous section. Furthermore, the proportionality to $1/T$ for both polymers agrees with Eq. 3-5. From the slope of the lines in Fig. 3-5, values of Λ were calculated to be -11.7 J/cm^3 for hemicellulose and -90.6 J/cm^3 for lignin calculated with $\bar{M}_n$ for molecular weight, and -12.3 J/cm^3 and -90.3 J/cm^3 with $\bar{M}_v$. Thus, the Λ values were the same for different molecular weight averages.

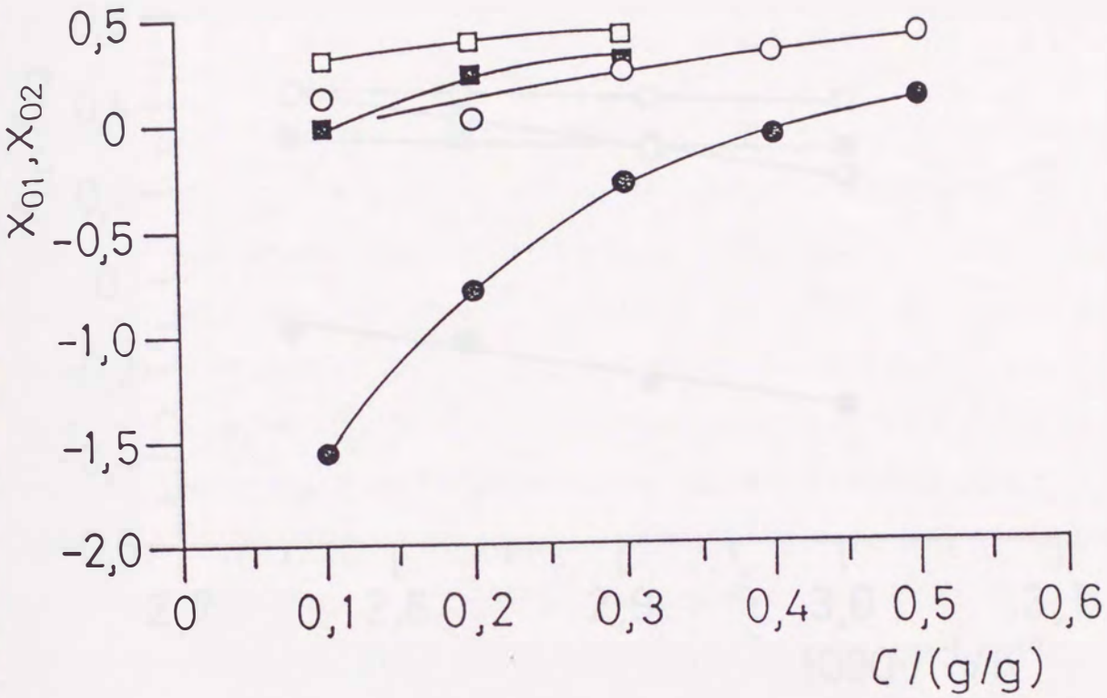

Fig. 3-4 Concentration dependence of interaction parameters of hemicellulose-DMSO (χ_{01}: □,■) and lignin-DMSO (χ_{02}: ○,●) at 60 °C. Open and closed symbols denote χ_{01} calculated from $\overline{M}_n$ and $\overline{M}_v$, respectively.

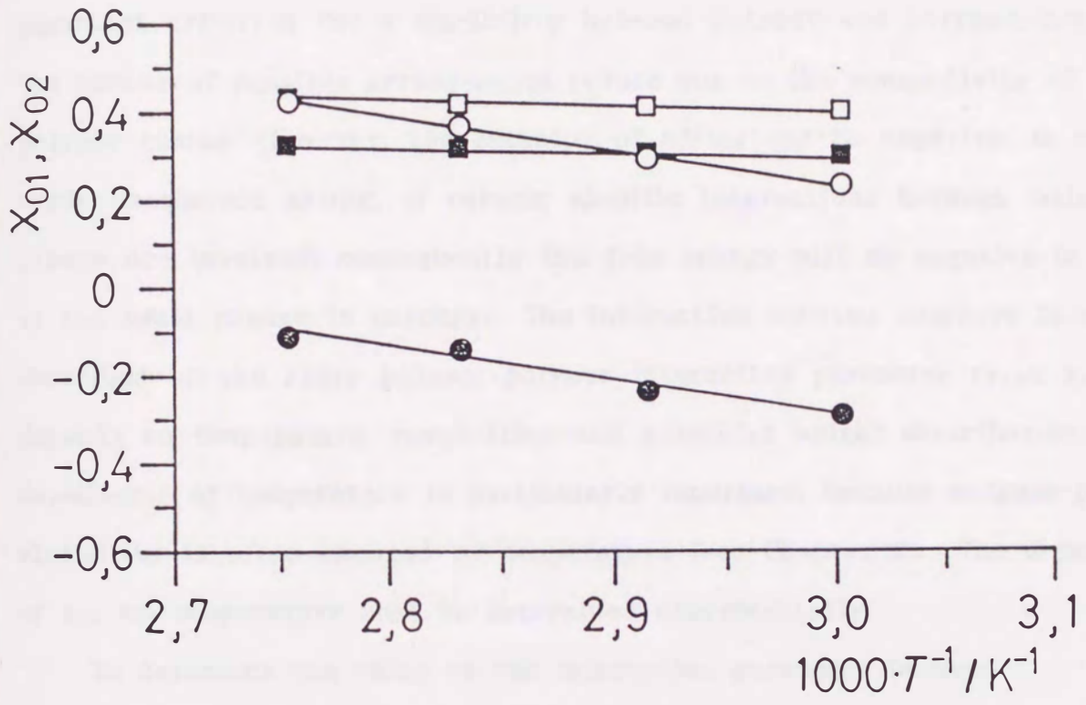

Fig. 3-5 Temperature dependence of interaction parameters of hemicellulose-DMSO (χ_{01}: □,■) and lignin-DMSO (χ_{02}: ○,●) at 0.3 g/g. Open and closed symbols denote χ_{01} calculated from $\overline{M}_n$ and $\overline{M}_v$, respectively.

3.3.3 *Interaction parameter between hemicellulose and lignin (χ_{12})*

Theory

According to Flory-Huggins theory [24], combinatorial entropy is not an important criterion for a miscibility between polymer and polymer, because the number of possible arrangements reduce due to the connectivity of polymer chains. However, the enthalpy of mixing can be negative, in other words exothermic mixing, if certain specific interactions between polar groups are involved; consequently the free energy will be negative in spite of the small change in entropy. The interaction between polymers is usually described by the Flory polymer-polymer interaction parameter (χ_{12}); χ_{12} depends on temperature, composition and molecular weight distribution. The dependence of temperature is particularly important, because polymer-polymer miscibility is often changed by temperature (see Chapter 2). The dependence of χ_{12} on temperature must be determined experimentally.

To determine the value of the interaction parameter between hemicellulose and lignin, χ_{12}, the activity in a ternary solution of solvent, hemicellulose and lignin was measured. According to Scott [70] and Tompa [71], the interaction parameter between solvent and polymers (χ^*) is described by an extension of the Flory-Huggins expression,

$$-\ln a_o = \ln v_o + (1-1/m_1)v_1 + (1-1/m_2)v_2 + \chi^*(v_1+v_2)^2, \qquad (3\text{-}6)$$

where subscripts 0, 1 and 2 indicate solvent (DMSO), polymer-1 (hemicellulose) and polymer-2 (lignin), respectively. By substitution of the values of a_o, v_i and m_i in Eq. 3-6, we obtain the parameter χ^*. The χ^* is related to χ_{o1} and χ_{o2} in binary solution by

$$\chi^{*} = (1-\xi)\chi_{o1} + \xi\chi_{o2} - \xi(1-\xi)\chi_{12}, \quad (3\text{-}7)$$

and

$$\xi = v_2/(v_1+v_2), \quad (3\text{-}8)$$

where ξ is the volume fraction of polymer-2 for polymers. Like the Flory-Huggins theory, Eq. 3-7 is not valid at low concentrations; therefore the following discussion is for data obtained at a concentration of 0.3 g/g.

Interaction parameter between hemicellulose and lignin

The temperature dependence of χ^{*} at ξ=0.505 calculated from $\bar{M}_n$ and $\bar{M}_v$ are shown in Fig. 3-6 (a) and (b), respectively. These figures include the data of χ_{o1} and χ_{o2} previously expressed in Fig. 3-5. Evidently, the change of χ^{*} is not linear to $1/T$. This observation cannot be expressed by Eq. 3-5, whereas the temperature dependence of χ_{o1} and χ_{o2} agrees with Eq. 3-5.

The interaction parameter between polymers (χ_{12}) was estimated from Eq. 3-7 by m_i based on each $\bar{M}_n$ and $\bar{M}_v$. The results are shown in Fig. 3-7. For the two molecular weight averages, both the absolute values and the trends in χ_{12} are identical. The value of χ_{12} varied widely from -0.036 to 0.551 for a narrow change of temperature. As shown in Fig. 3-7, there is a pronounced minimum in χ_{12} at around 70 - 80 ˚C at which temperature the interaction parameter is negative. On either side of the minimum, χ_{12} becomes positive. This indicates a net attractive force between lignin and hemicellulose in DMSO at 70 - 80 ˚C, while at higher and lower temperatures repulsion forces predominate.

Dambis *et al.* [5] have calculated the isotherm solubility parameters (δ) of the three main cell wall components of wood with and without due account for hydrogen bonding. They have shown that δ with hydrogen bonding

was 12.6 $(cal/cm^3)^{1/2}$ for *O*-acetyl-4-*O*-methylglucuronoxylan, and 10.1 - 11.3 $(cal/cm^3)^{1/2}$ for lignin. It was also found that the δ value of the hemicellulose was decreased with increase of content of acetyl groups in the molecule. The δ values for hemicellulose and lignin was close; this was unexpected because of differences in their molecular structures. Therefore, the authors have suggested that the lignin and hemicellulose may be partially miscible in domains where the content of acetyl groups is higher than average. By substitution of the values of δ in $\chi_{12}=V_o/RT(\delta_1-\delta_2)^2$, χ_{12} is calculated to be 0.048 - 0.179 at 25 ˚C. This positive value is in general agreement with the present result. However, there is no information on temperature dependence from their results.

In most polymer systems, the χ_{12} decrease with an increase in temperature. In the present work the behavior of hemicellulose and lignin between 60 ˚C and 70 ˚C agrees with this trend. However above 70 ˚C, χ_{12} goes through a minimum and then increases. This apparently anomalous behavior may be due to the hydrogen bonding. Remko and Polčin [81] studied the interaction between hemicellulose and lignin by using the 'Perturbative Configuration Interaction using Localized Orbitals' method for model complexes. They postulated that stable complexes exist, with the carboxyl group acting as a proton donor. If so, χ_{12} would increase with temperature, because the strength of hydrogen bonding is decreased by increase in temperature. Therefore, it may be that the minimum in χ_{12} shown in Fig. 3-7 is the result of competition between normal decreasing trend given by Eq. 3-5 and an increase caused by the weakening of the hydrogen bonding with an increase in temperature.

Miscibility for polymer-polymer blends is expected when χ_{12} is negative or very small. Usually χ_{12} decreases slightly with an increase in

temperature for mixtures near the upper critical solution temperature (UCST). In contrast, the parameter slightly increases near the lower critical solution temperature (LCST). If χ_{12} goes through a minimum with temperature, the blends have a phase diagram of UCST+LCST or the hourglass type. From the results shown in Fig. 3-7, binary blends of hemicellulose and lignin are predicted to be miscible at 70 - 80 ˚C and to have UCST+LCST or hourglass type of phase diagrams. However, this behavior cannot be demonstrated experimentally because of the high glass transition temperatures of the woody polymers; as shown in Chapter 2, *Tg* values for hemicellulose and lignin are 210 ˚C and 131 ˚C, respectively. At above 90 ˚C, hemicellulose and lignin were found to be immiscible in attempts to cast blends into film. This result agrees with the trends in χ_{12} shown in Fig. 3-7.

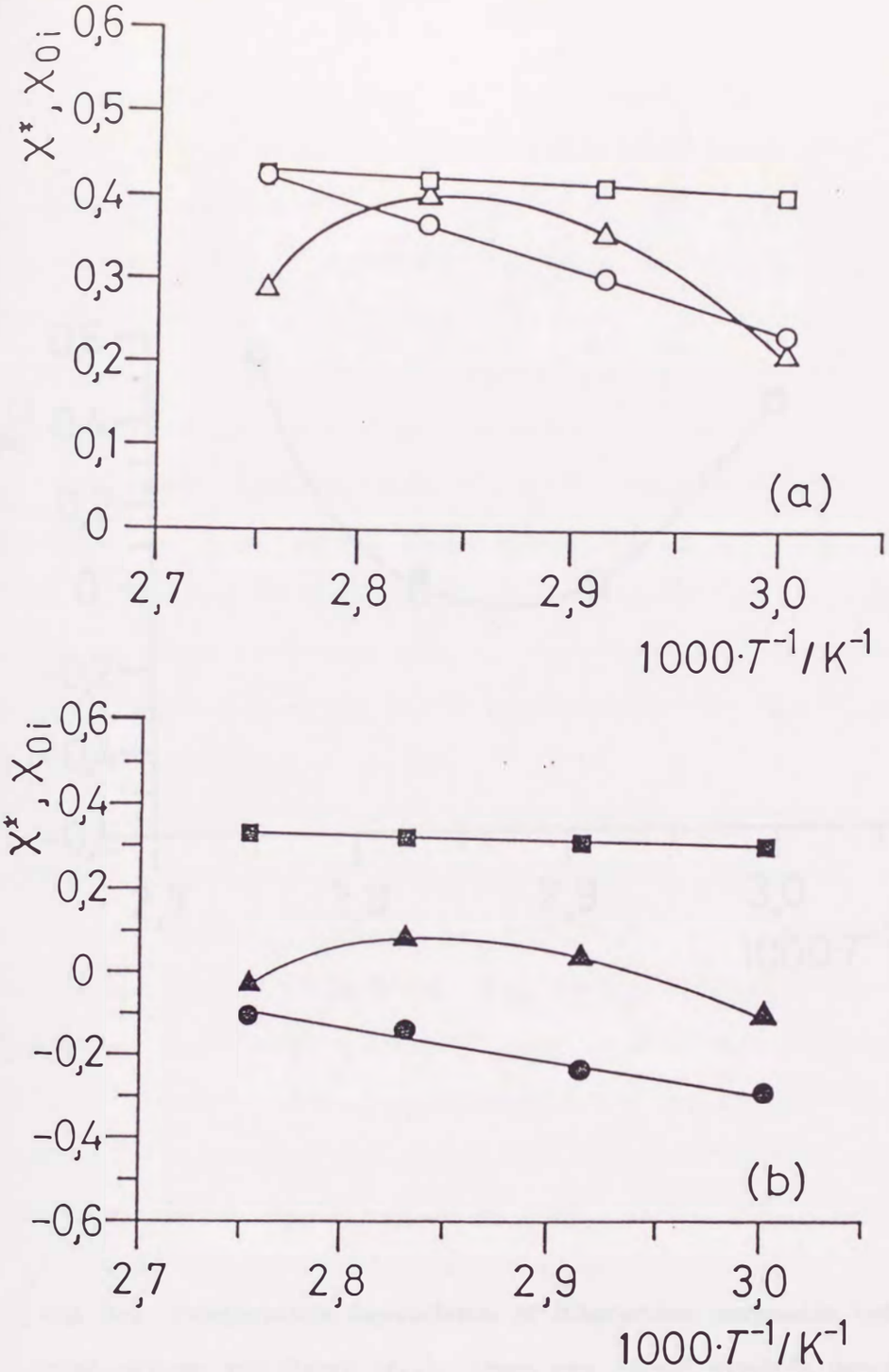

Fig. 3-6 Temperature dependence of interaction parameters between solvent-polymers (χ^*: △,▲) calculated from (a) $\overline{M}_n$ and (b) $\overline{M}_v$. The data for χ_{o1} and χ_{o2} in Fig. 3-5 are included.

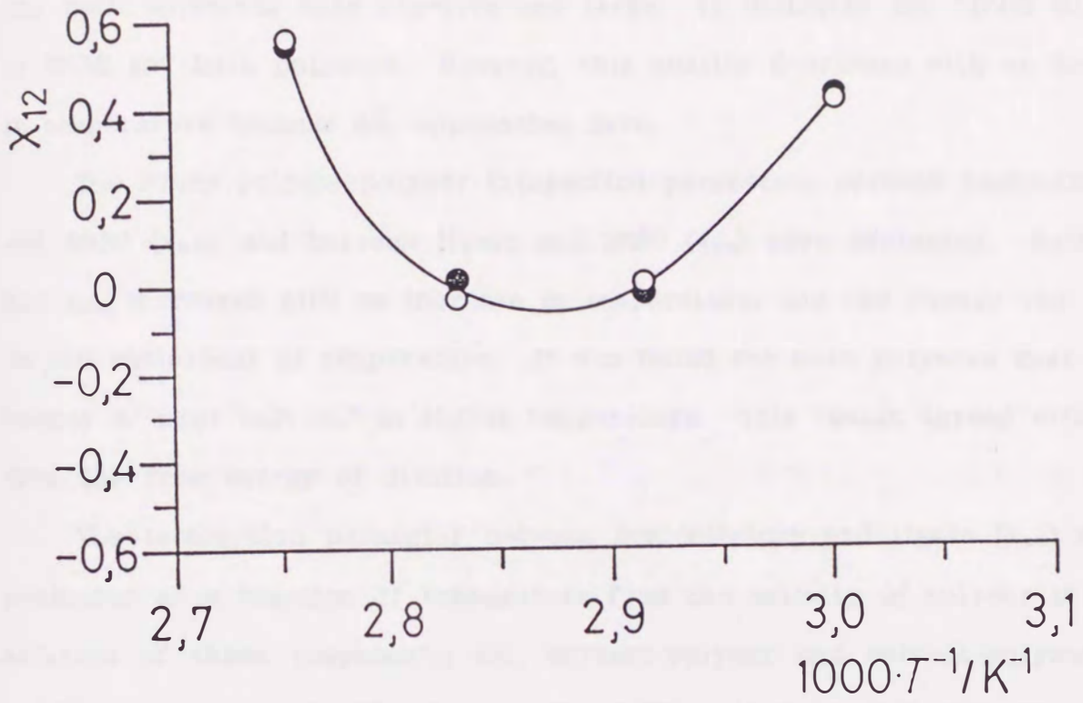

Fig. 3-7 Temperature dependence of interaction parameter between hemicellulose and lignin (χ_{12}). Open and closed symbols denote the χ_{12} calculated from $\overline{M}_n$ and $\overline{M}_v$, respectively, with from Eq. 3-6 to 3-8. Concentration is 0.3 g/g and the volume fraction of lignin for polymers (ξ) is 0.505.

3.4 Conclusion

The solution properties of hemicellulose and lignin from beech wood in dimethylsulfoxide (DMSO) was investigated by vapor pressure osmometric measurement (VPO). It was found that the free energies of dilution ($\Delta\bar{G}_o$) of the both solutions were negative and large. It indicates the "good solvent" of DMSO for both polymers. However, this quality decreased with an increase in temperature because $\Delta\bar{G}_o$ approaches zero.

The Flory polymer-polymer interaction parameters between hemicellulose and DMSO (χ_{o1}), and between lignin and DMSO (χ_{o2}) were evaluated. Both χ_{o1} and χ_{o2} increased with an increase in temperature, and the change was linear to the reciprocal of temperature. It was found for both polymers that DMSO become a "poor solvent" at higher temperature. This result agreed with one from the free energy of dilution.

The interaction parameter between hemicellulose and lignin (χ_{12}) was evaluated as a function of temperature from the activity of solvent in a solution of three components; *i.e.*, solvent-polymer and solvent-polymer-polymer solutions. At 60 ˚C, χ_{12} was positive; it decreased with an increase in temperature and became negative at 70 - 80 ˚C where there was a minimum. Above 80 ˚C, χ_{12} again increased to become positive at 90 ˚C. Thus, hemicellulose and lignin have been shown to interact strongly with each other in the temperature range of 70 - 80 ˚C. At higher or lower temperature, interpolymer repulsion exceeds attraction.

Chapter 4

Surface Tension Studies on Hemicellulose and Lignin Blends

4.1 Introduction

Most small-molecule organic liquids are mutually miscible and their mixtures do not form stable interfaces. Polymers are, however, usually immiscible and their mixtures form multiphase structures with stable interfaces. The dispersion, morphology, and adhesion of the component phases are greatly affect by the interfacial energies, which thereby play an important role in determining the mechanical properties of a multiphase polymer blend. The behavior of phase-separated polymer systems is governed to a large extent by the interfacial properties [82].

Surface tensions, interfacial tensions, and contact angles can be used as laboratory tools for the evaluation of the various intermolecular forces that determine cohesion in a single phase or adhesion between two dissimilar materials at an interface. By the use of these tools, considerable information about the magnitude of various intermolecular forces may become available [82].

Despite its importance, reliable measurements of the interfacial tension between polymers (γ) have not been reported until 1969 because of the experimental difficulty in handling highly viscous polymer melts. A measurement of γ is very difficult, but some results have been reported. In these, γ of the mixture of two homopolymers was measured in melting condition by drop method [83]. On the other hand, the surface tension of

solid polymer may also be evaluated indirectly from wettability data. Many methods have been proposed, for example, calculations are based on emprical or semiemprical relations between the surface tension and the contact angle [84,85].

In Chapter 2, the miscibility between hemicellulose and lignin in *bulk phase* was evaluated by means of DSC, but information as to the *surface states* of the hemicellulose and lignin blends is not yet obtained. To examine the miscibility at the surface of the blend solid, the surface tension was investigated by measurements of contact angle of different liquids. First, the dependence of the *critical surface tension* on blending ratio was observed by using of Zisman plot. Next, the *dispersion and polar contributing forces* in surface tension and the *surface tension of solid* was estimated based on the Owens' equation. Further, the heterogeneity of surface examined by measurements of the *advancing and receding contact angles* on tilted plane.

4.2 Experimental

4.2.1 *Materials*

Hemicellulose and lignin were prepared from wood meal of beech (*Fagus crenata* Bl.) as described in Chapter 1.

1,2-propanediol, 1,3-buthanediol and glycerol were reagent grade (Wako Pure Chemical Industries, Ltd., Japan) and used for wetting liquid. The surface tension values of the respective liquids were sited from literature [86]. The values of the dispersion and polar contributing forces of surface tension were estimated for these liquids by the measurement of contact angle on polytetrafluoroethylene solid [87].

4.2.2 *Preparation of blend films*

0.2 ml of 5 % sample solution in DMSO was spread on a thin cover glass for microscope. The solvent was removed by drying at 60 ˚C for 24 hours in vacuo.

4.2.3 *Measurement of contact angle*

There are several methods for the measurement of contact angles, but the most widely used method is to measure the angle of a drop resting on a solid surface with the aid of a microscope having an angle-measuring eyepiece, as illustrated in Fig. 4-1. A drop of 5-15 μl was placed on the sample film, and its contact angle was measured with a contact angle meter (Erma Model G-III, Japan) at 25 ˚C and 5 min of waiting time. The data were obtained by averaging the results as ten or more measurements.

4.3 Results and Discussion

4.3.1 *Critical surface tension*

Consulting the literature [84], the degree to which a liquid wets a solid is measured by the contact angle (θ). Figure 4-1 shows the schematic diagram of liquid drop on solid surface and acting of surface tensions. When θ=0, the liquid spreads freely over the surface and is said to completely wet it. Complete wetting occurs when the molecular attraction between the liquid and solid is greater than that between similar liquid molecules [88]. At incompletely wetting, the surface tensions are related to the contact angle by an expression from equilibrium considerations.

$$\gamma_{SV} = \gamma_{SL} + \gamma_{LV} \cos \theta, \qquad (4\text{-}1)$$

where γ_{SV} = solid-vapor surface tension; γ_{SL} = solid-liquid surface tension; and γ_{LV} = liquid-vapor surface tension. However, the liquid surface tension is little affected by the vapor phase, so that $\gamma_{LV} \approx \gamma_L$. The surface tension of a solid that has adsorbed a layer of vapor, γ_{SV}, is related to the surface tension of solid, γ_S, as $\gamma_{SV} = \gamma_S - \pi_e$. The π_e is the reduction term of γ_S resulting from vapor adsorbed on the solid surface. The value of spreading pressure, π_e, in the above equations is very often zero, although there are a few systems in which π_e must be taken into consideration.

A widely-used method for determining the surface tension of a solid was developed using contact angle measurements. It is well known the "Young's equation" [89]. A plot of cos θ against the surface tension, γ_L, for homologous series of liquids can be extrapolated to give a critical surface tension (γ_C) at which cos θ = 1. Any liquid with a surface tension less than γ_C completely wets the solid surface. The critical surface tension,

γ_c, has therefore been taken widely, but not exactly, as a measure of the surface free energy, γ_s, of the solid.

Figure 4-2 shows the typical examples called the Zisman plot [90,91]; γ_L is plotted against cos θ for 1,2-propanediol, 1,3-butanediol and glycerol on the surfaces of hemicellulose, lignin and their mixture (50:50). Since these liquids dissolve neither hemicellulose nor lignin, these liquids can be used for a contact angle measurement. γ_c values obtained from the Zisman plots were 32.2 and 34.1 dyne/cm for hemicellulose and lignin, respectively. These values agreed with literatures [92,93]; γ_c = 34 dyne/cm for hemicellulose, 36 dyne/cm for some lignins. It is noted that the γ_c values of hemicellulose and lignin are closed each other, although they are different in chemical composition, especially hydrophobicity.

Figure 4-3 shows the γ_c at various blending ratios. The values of γ_c in the blends are found between those of hemicellulose and lignin and likely to have a linear relation. It indicates the surfaces of blends are similar at any blending ratio, while the miscibility in bulk phase apparently depends on blending ratio (see Chapter 2).

It should be noted, however, that the precise value of γ_c is generally dependent on the particular series of liquids used to determine it. A series of polar liquid, such as alcohols, will give a higher γ_c than a series, such as simple hydrocarbons, which interacts less strongly with the same surface [94]. Moreover, the value of γ_c is a measure of the wettability for a series of liquids used, and γ_c reflects complex interaction parameters such as γ_{sv}, γ_{sL} and π_e in Eq. 4-1. So, there is less information about intermolecular interactions of blended polymers.

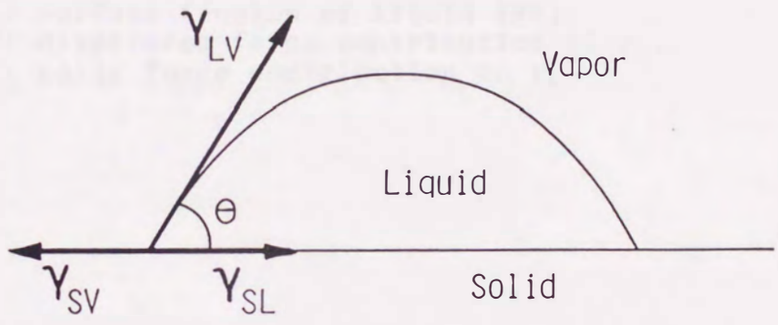

Fig. 4-1 Schematic diagram of liquid drop on solid surface and acting of surface tensions.

γ_{sv}: solid-vapor surface tension.

γ_{sL}: solid-liquid surface tension.

γ_{Lv}: liquid-vapor surface tension.

θ : contact angle.

Table 4-1 Surface tension of used liquids.

	Surface tension (dyne/cm)		
	γ_L	γ_L^d	γ_L^p
1,2-propanediol	36.5	24.5	12.0
1,3-butanediol	37.8	22.6	15.2
glycerol	63.0	37.4	26.0

γ_L : surface tension of liquid [86].
γ_L^d: dispersion force contribution to γ_L.
γ_L^p: polar force contribution to γ_L.

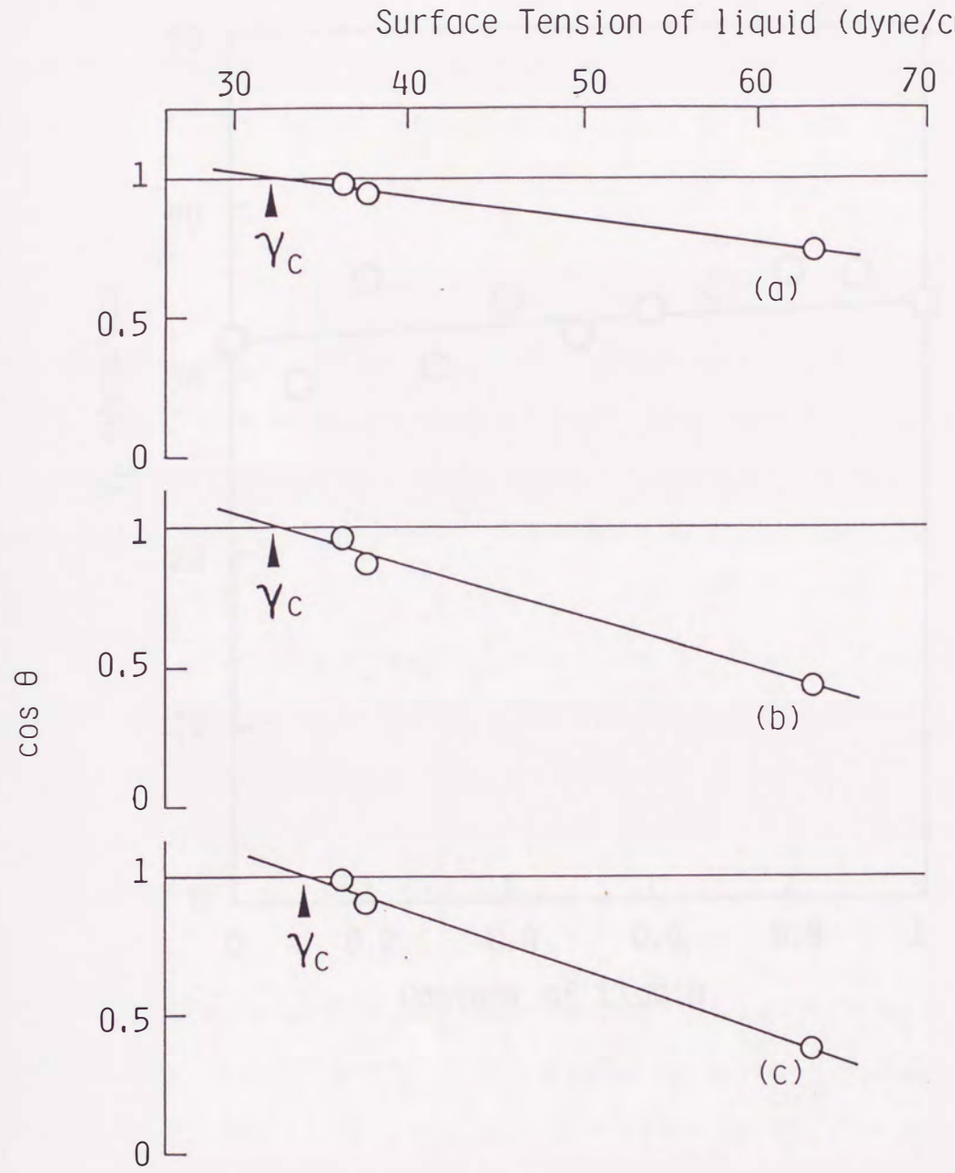

Fig. 4-2 Zisman plots for (a) hemicellulose, (b) mixture (50:50) and (c) lignin.

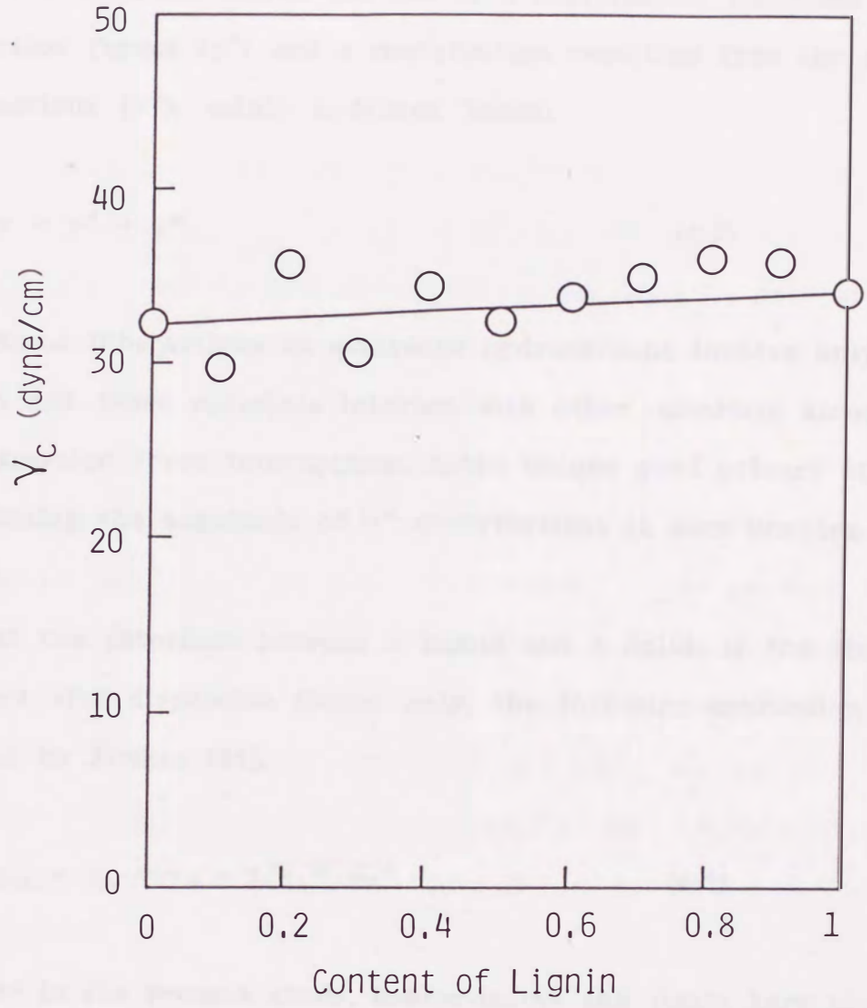

Fig. 4-3 γ_c of hemicellulose and lignin blends obtained by Zisman plots.

4.3.2 *Surface tension of solid (γ_S)*

In the case of the surface tension of a liquid, *e.g.* water, the surface tension can be considered the sum of a contribution resulting from dispersion forces (γ^d) and a contribution resulting from the polar interactions (γ^p), mainly hydrogen bonds:

$$\gamma = \gamma^d + \gamma^p. \qquad (4\text{-}2)$$

Since interactions in saturated hydrocarbons involve only dispersion forces and these materials interact with other materials almost exclusively by dispersion force interactions, these become good primary standards for determining the magnitude of γ^d contributions in more complex liquids and solids.

At the interface between a liquid and a solid, if the liquid and solid interact with dispersion forces only, the following expression has been derived by Fowkes [84],

$$\gamma_{SL} = \gamma_L + \gamma_S - 2\sqrt{\gamma_L^d \cdot \gamma_S^d}. \qquad (4\text{-}3)$$

However in the present study, hemicellulose and lignin have some hydroxyl groups; this implies that not only dispersion forces but also polar contributing forces should be taken into account.

Girifalco *et al.* [95], Hata *et al.* [87,96] and Owens *et al.* [97] have shown an expression of the surface tension of solid involving both dispersion and polar forces by expanding the Fowkes' equation, as follows

$$\gamma_{Lv}\,(1 + \cos\,\theta) = 2\sqrt{\gamma_S^d \cdot \gamma_L^d} + 2\sqrt{\gamma_S^p \cdot \gamma_L^p}, \qquad (4\text{-}4)$$

where

$$\gamma_{SV} = \gamma_S^d + \gamma_S^p \approx \gamma_S, \qquad (4\text{-}5)$$

$$\gamma_{LV} = \gamma_L^d + \gamma_L^p \approx \gamma_L. \qquad (4\text{-}6)$$

Equation 4-4 shows that if we measure the contact angles of two or more liquids whose γ_{LV}, γ_L^d and γ_L^p are already known on a given solid surface, the dispersion force contribution to surface tension, γ_S^d, and the polar force contribution, γ_S^p, are able to be determined for the solid surface. If we obtain the γ_S^d and γ_S^p of the polymer surface, γ_S is determinable from the relation $\gamma_S = \gamma_S^d + \gamma_S^p$ (Eq. 4-5).

The pair of water and methylene iodide are usually used as wetting liquids to obtain γ_S^d and γ_S^p. Nevertheless in the present study, water is not applicable because water causes swelling of hemicellulose. Moreover, methylene iodide is not usuable; Ray *et al.* suggested that there exists some specific affinity of iodide for OH groups [98]. Instead of water and methylene iodide, therefore, 1,2-propanediol and 1,3-butanediol were employed for the present work. The γ_L^d and γ_L^p values of diols are listed in Table 4.1.

For each wetting liquid, the known γ_L value and the observed θ value at each mixing ratio of blend were substituted into the left hand side of Eq. 4-4, while the known values of γ_L^d and γ_L^p are substituted into the right hand side. Thus, we could solve two simultaneous equations in two unknowns, γ_S^d and γ_S^p, at each mixing ratios. Figure 4-4 shows the γ_S^d, γ_S^p and γ_S of the blend surface of hemicellulose and lignin as a function of mixing ratio. In the figure, open circles and open squares denote γ_S^d and γ_S^p, respectively, and filled circles denote γ_S which is sum of γ_S^d and γ_S^p.

Looking at the data of homopolymers, γ_s^p of hemicellulose is larger than that of lignin, while γ_s^d is contrast. The larger γ_s^p for hemicellulose indicates that the hydrophilicity of hemicellulose is stronger than that of lignin, on the other hand lignin has larger γ_s^d, this means the stronger hydrophobicity of lignin. And also, Figure 4-4 indicates that the total surface tension of solid, γ_s, is independent of blending ratio or may be in agreement with the linear relation within experimental error. The scattering of γ_s^d and γ_s^p may result from the history of samples examined, *i.e.*, the measured points depend on the preparation process, or especially on the duration after the blend treatment. As to γ_s, the trend to the change with blending ratio seems similar to that of γ_c. This similarity is represented by the knowledge that the γ_s is nearly equal to γ_c. However, the absolute values of γ_s are larger than γ_c.

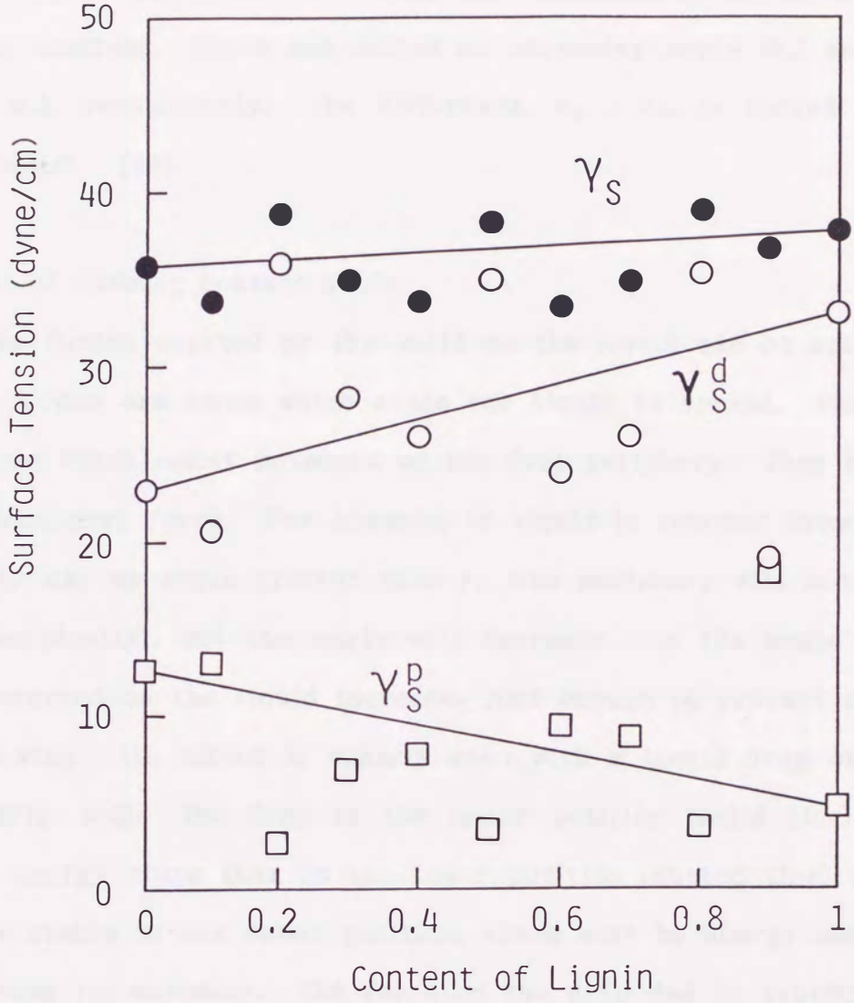

Fig. 4-4 Dispersion force (γ_s^d), polar force (γ_s^p) and total surface tension (γ_s) of blends of hemicellulose and lignin.

4.3.3 *Dynamic contact angles*

It is found that for a given liquid-solid system, a number of stable angles can be measured. Two relatively reproducible angles are the largest and the smallest. These are called an advancing angle (θ_a) and a receding angle (θ_r), respectively. The difference, $\theta_a - \theta_r$, is called the "*hysteresis*" [85].

Concept of dynamic contact angle

The forces exerted by the solid on the liquid can be active or passive. Active forces are those which cause the liquid to spread. Passive forces are those which resist movement of the drop periphery. They behave formally as a frictional force. For example, if liquid is removed from a drop which initially has an angle greater than θ_r, the periphery will not move (macroscopically), but the angle will decrease. As the angle decreases, the force exerted on the liquid increases just enough to prevent the periphery from moving. Its effect is clearly seen with a liquid drop on a tilted plate (Fig. 4-5). The drop in the upper position (solid line) is in a higher energy state than in the lower position (dotted line). Since the drop is stable in the upper position, there must be energy barriers preventing its movement. The force on the drop due to gravity is $mg \cdot \sin \alpha$, where m is the mass of the drop and α is the tilt angle. This body force must be balanced by the surface forces around the periphery. Rosano [99] and Furmidge [100] have shown the situations by the equation,

$$mg \cdot \sin\alpha = w\ \gamma_{LV}(\cos\ \theta_R - \cos\ \theta_A), \qquad (4\text{-}8)$$

where w is the width of the drop, θ_A refers to the contact angle at the

leading edge, and θ_R the angle at the rear. If α is not at its maximum value, the plate can be tilted still further and the drop will remain stationary. The force from gravity will increase by $mg \cdot \Delta\sin\alpha$. The contact angle θ_A and θ_R will adjust themselves to compensate for this force increase. When they become the advancing and receding angles, respectively, the drop will no longer be able to adjust itself and will roll off the plate. If there were no hysteresis, the drop would roll off at the slightest tilt of the plate.

If a surface is rough, the apparent (macroscopic) contact angles measured with respect to the tilt plane are different at the front and rear while the front and rear edges both meet the solid with the same intrinsic (microscopic) angle. Furthermore, surface heterogeneity can also cause hysteresis. Consider the surface having high- and low-contact-angle regions. As a drop periphery advances over such a surface, the edge of the liquid tends to stop at the boundaries of the high-energy islands. About this situation, Pease [101] suggested that advancing angles should be associated with the intrinsic angle of the high-contact-angle regions of surface. Similarly, receding angles should be associated with low-contact-angle areas.

Johnson and Dettre have analyzed the relationship between hysteresis of contact angle and the surface heterogeneity by specific model system [85]. The several qualitative conclusions which are useful in interpreting experimental data are

1) Advancing angles are more reproducible on predominantly low-energy surfaces whereas receding angles are more reproducible on predominantly high-energy surfaces.

2) Advancing contact angles alone are not a reliable measure of surface

coverage. Thus, 10 and 90 % coverage (by a low-energy monolayer say) give about the same advancing angle. Similar considerations apply for receding angles.

3) An advancing angle is a good measure of the wettability of the low-energy part of the surface and a receding angle is more characteristic of the high-energy part.

As shown above, dynamic contact angles are a good measure of heterogeneity of surface [102,103]. Since present system is mixture of hydrophylic (hemicellulose) and hydrophobic (lignin) polymers, the hysteresis of contact angle is a measure of heterogeneity for blend surface.

Blends of hemicellulose and lignin

Figure 4-6 shows the change of measured contact angles with increase in plane angle. Glycerol was employed as a liquid. For hemicellulose surface, a contact angle was 42° at horizontal plane. The advancing angle (θ_a) increased with increasing of plane angle (α). Conversely the receding angle (θ_r) decreased with α. Increasing of θ_a means that the development of drop by gravity is resisted by balance of surface tensions (γ_{SV}, γ_{SL} and γ_{LV}). With further increase of α, θ_a and θ_r showed the steady values which were identical to θ_A and θ_R, respectively.

Figure 4-7 shows the θ_A and θ_R of glycerol drop as a function of mixing ratio. It is noteworthy that a constancy in θ_A data of mixed systems and an accordance with the value of lignin are found. This indicates that a kind of adsorption of lignin takes place at the air-solid interface during the process of solidification from gel state, since lignin is more hydrophobic compared with hemicellulose, so that lignin favors more the air-solid interface. This adsorption phenomenon is observed at any mixing ratio.

Looking at the θ_R data, the data for mixed systems also are likely to be constant in between θ_R values of respective pure systems, but a little bit higher than that of pure hemicellulose. This slight increase in θ_R is also interpreted to be caused by the increase in lignin/hemicellulose ratio at the surface compared with the bulk phase of the polymer mixture.

Figure 4-8 shows the diagram of the hysteresis, $\theta_A - \theta_R$, against mixing ratio. The hysteresis was 32° for hemicellulose, 27° for lignin, and ca. 40-45° for their mixtures. It is noteworthy that the hysteresisses of mixtures are larger than those of homopolymers and seem to be constant. This result indicates that the heterogeneity at mixture the surface is larger than at homopolymers and it is independent of mixing ratio.

The figures clearly tell us that the surface states of the mixture is governed mainly by the more hydrophobic species even though the mixing ratio is changed. This interesting finding suggests that the present surface tension method does not reflect the bulk phase property, that is, this method is not applicable for estimate of cohesion in bulk phase when a solid material is produced from solution of two or more components whose hydrophobicities are quite differnet from each other, and also the composition of surface phase is not same as that of bulk phase. The bulk or gross properties such as cohesion between polymer molecules should be evaluated from different methods such as shown in Chapter 2.

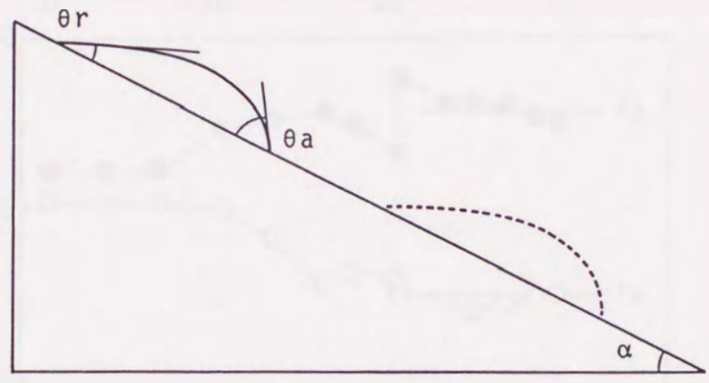

Fig. 4-5 Schematic diagram of contact angles on tilted plane.

α : angle of tilted plane.

θ_a: advancing contact angle.

θ_r: receding contact angle.

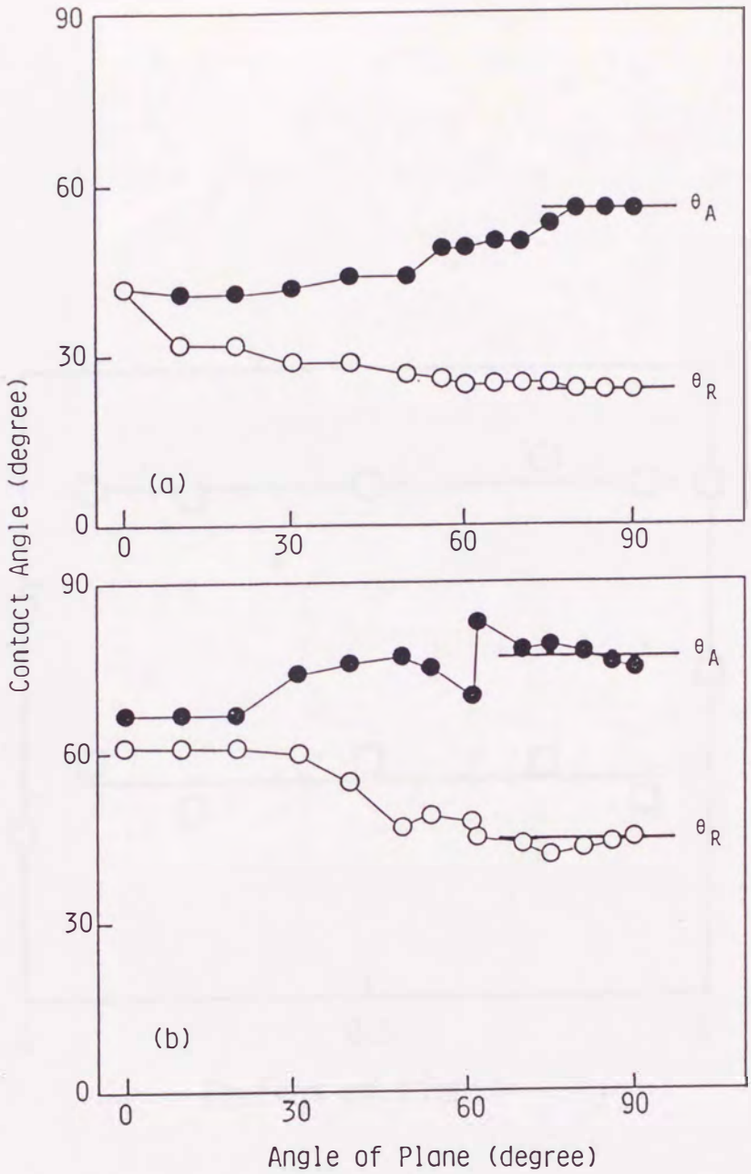

Fig. 4-6 Dynamic contact angles of glycerol drop on the surface of (a) hemicellulose and (b) lignin. Filled and open circles denote the advancing (θ_a) and receding (θ_r) contact angles. Steady values with increasing of plane angle are identical to θ_A and θ_R.

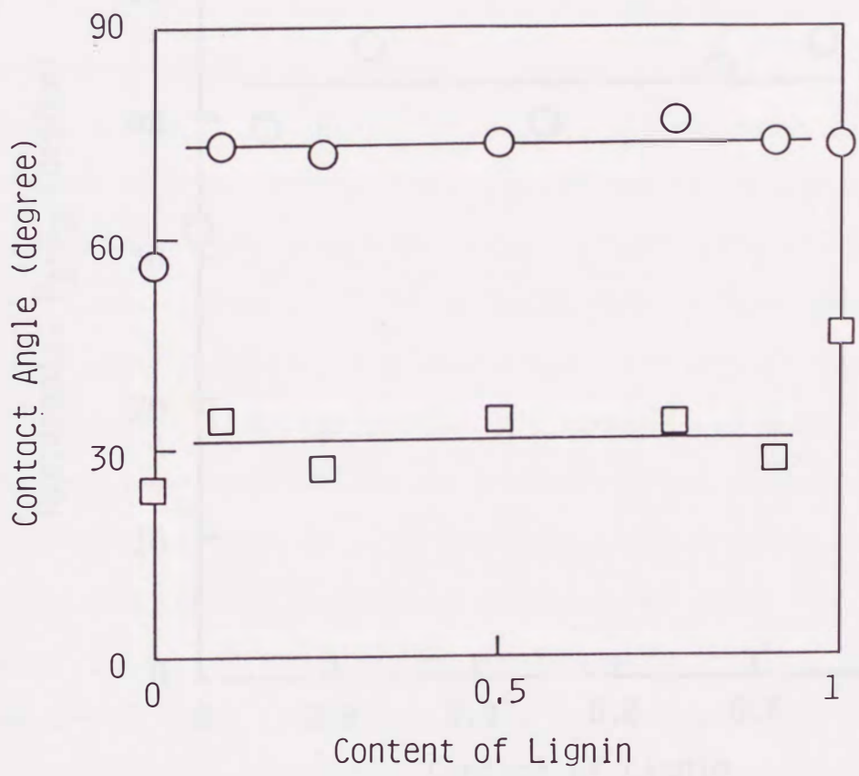

Fig. 4-7 The diagram of θ_A (○) and θ_R (□) *vs.* mixing ratio.

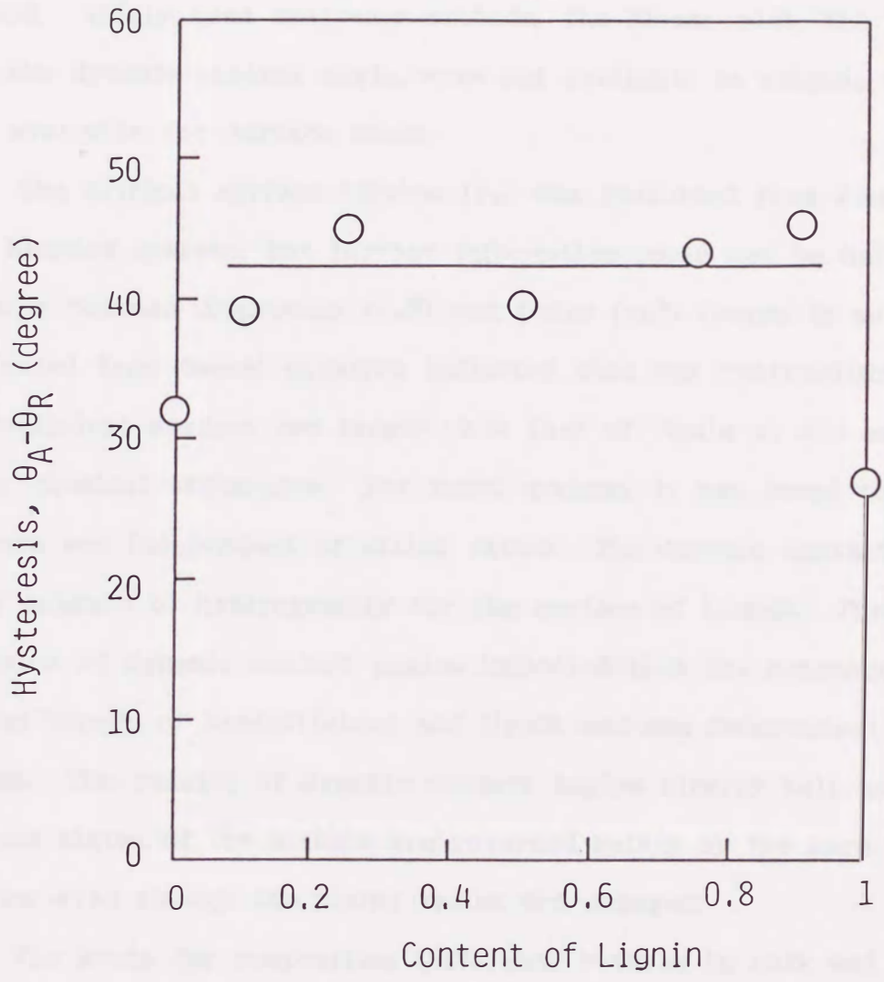

Fig. 4-8 The diagram of hysteresis, θ_A - θ_R, *vs.* mixing ratio.

4.4 Conclusion

The miscibility between hemicellulose and lignin was investigated from the behavior in surface tension of solid determined by a contact angle method. Widely used analysing methods, the Zisman plot, the Owens' equation and the dynamic contact angle, were not available to examine the bulk state but available for surface state.

The critical surface tension (γ_c) was evaluated from Zisman plot for the blended systems, but further information could not be derived. The balance between dispersion (γ_s^d) and polar (γ_s^p) forces in surface tension evaluated from Owens' equation indicated that the hydrophilicity of hemicellulose surface was larger than that of lignin as was expected from their chemical structures. For mixed systems, it was found that the blend surface was independent of mixing ratios. The dynamic contact angle was a good measure of heterogeneity for the surface of blends. The hysteresis behavior of dynamic contact angles indicated that the heterogeneity occurred in the blends of hemicellulose and lignin and was independent of mixing ratios. The results of dynamic contact angles clearly tell us that the surface states of the mixture are governed mainly by the more hydrophobic species even though the mixing ratios are changed.

The study for composition difference between in bulk and in surface should be important to the application of woody materials, *e.g.*, the blends of cellulose derivative and functional polymer, the wood derivatives involving both polysaccharides and lignin, etc.

Summary

The purpose of this research is to estimate the degree of interaction between cellulose, hemicellulose and lignin isolated from wood cell wall and also the effect of their copolymer, lignin-carbohydrate complex (LCC), on the interaction. For this purpose, some investigations were performed; the interfacial adhesion of those polymer layers, the miscibility of polymer blends by means of the observation of their glass transition temperatures; the solution properties of hemicellulose and lignin; the cohesive forces of polymer molecules in solid surface by a surface tension. These discussions were carried out from the viewpoint of the Flory polymer-polymer interaction parameter between polysaccharide and lignin (χ_{12}).

In Chapter 1, to determine the adhesion for the different pairs among cellulose, hemicellulose and lignin, the interlaminar bond strength (σ) was measured. The σ was strong for a cellulose/hemicellulose pair, but weak for cellulose/lignin and hemicellulose/lignin pairs. However, the σ between cellulose and lignin was enhanced by adding LCC. Further, it was more enhanced by the LCC situated at interface than that mixed in lignin lamina. From the measurements of the contact angle of liquid drop, it was found that the LCC molecules spread on cellulose surface oriented their lignin part to air side and polysaccharide part to cellulose side. These results indicate that the LCC works as an adhesive or a surfactant. The enhancement of σ by a LCC of nearly equal proportion of polysaccharide and lignin in LCC molecules was stronger than those of lignin-rich or polysaccharide-rich compositions of LCCs. It has been found that LCC works as a compatibilizer between cellulose and lignin from observation by the tensile strength of

solution casted film [16]. Present results proved this behavior, *i.e.*, the adhesion of interface of cellulose and lignin was enhanced by small amount of LCC.

In Chapter 2, the miscibility between hemicellulose and lignin from hardwood was determined by differential scanning calorimetry. The glass transition temperature (*Tg*) was measured as a function of mixing ratio. The binary-blends of these polymers were separated into two phases showing two *Tg*s in a wide range of blending ratios. However, the *Tg*s of hemicellulose and lignin were getting close to the another *Tg* with blending of another polymer. Therefore, it is suggested that this binary-blends system is partially miscible. Based on this suggestion, the composition ratios in each phase were calculated from the values of *Tg*s by Kim and Burns's equation. It appeared that the polymers mutually dissolved to another polymer-rich phase. The value of the interaction parameter between them (χ_{12}) was evaluated to 0.144 - 0.224; it decreased with an increase of lignin content. This result shows that the miscibility is comparatively better at hemicellulose-rich surrounding than at lignin-rich one.

In the ternary-blends system in which the LCC was added to the above system, the *Tg* of hemicellulose became indistinct, suggesting that the system approached to miscibility. Furthermore, after the quenching treatment with heating at 120-160 ˚C followed by rapid cooling at -25 ˚C, only one *Tg* was observed for the ternary-blends system, indicating the system became completely miscible. Particularly, the sample was miscible at lower heating temperature with increased addition of LCC. Based on these results, it was concluded that the binary system of hemicellulose and lignin is immiscible, but becomes miscible at high temperature by the addition of LCC. This observation suggests that the LCC works as a compatibilizer.

The binary- and ternary-blends systems of hemicellulose, lignin and LCC were changed from immiscible to miscible by increasing temperature. This behavior shows that this blends system has an "upper critical solubility temperature (UCST)" type composition-temperature phase diagram. But UCST could not be observed because of the decomposition of polymers. Also the value of χ_{12} was evaluated from the phase diagram. It was found that the χ_{12} decreased with temperature as well as the content of lignin. Estimated experimental equation was

$$\chi_{12} = (-0.085 + 130/T) + (0.25 - 160/T)\Phi_L,$$

where T is temperature in K and Φ_L is overall lignin fraction in the blends.

In Chapter 3, the interaction parameter between hemicellulose and lignin was evaluated from vapor pressure osmometric measurement for the solvent-polymer and solvent-polymer-polymer solutions. Dimethylsulfoxide (DMSO) was used as the solvent. The interaction parameters between hemicellulose and DMSO (χ_{01}) and between lignin and DMSO (χ_{02}) increased with increase in temperature, and the change of χ_{01} and χ_{02} was linear to reciprocal temperature. It was found for both polymers that DMSO became a "poor solvent" at higher temperatures. This result was also derived from the free energy of dilution. The interaction parameter between hemicellulose and lignin (χ_{12}) was evaluated as a function of temperature from the activity of solvent in a solution of three components. At 60 ˚C, χ_{12} was positive; it decreased with increase in temperature and became negative and showed a minimum at 70 - 80 ˚C. Above 80 ˚C, χ_{12} again increased to become positive at 90 ˚C. Thus, hemicellulose and lignin attracted each other at 70 - 80 ˚C, but there was repulsion between the polymers at higher and lower temperatures.

In the final chapter, the miscibility in surface between hemicellulose

and lignin was investigated from the behavior in surface tension of solid determined by a contact angle method. The critical surface tension (γ_c) was evaluated from the Zisman plot for the blended systems, but further information could be derived. The balance between dispersion (γ_s^d) and polar (γ_s^p) forces in surface tension evaluated from Owens's equation indicated that the hydrophilicity of hemicellulose surface was larger than that of lignin as expected from their chemical compositions. For the mixed systems, it was found that the surface state was independent of mixing ratios. The hysteresis behavior of dynamic contact angles indicated the heterogeneity occurred in the blends of hemicellulose and lignin and was independent of mixing ratios. The results of dynamic contact angles showed that the surface states of the mixture are governed mainly by the more hydrophobic species even though the mixing ratios are changed.

In conclusion, the present study proved that polysaccharide and lignin had a poor affinity to each other as was expected from their chemical structures. However, LCC was found to work as a compatibilizer (a surfactant or an emulsifier) between them. Since cellulose, hemicellulose and lignin have a laminated structure in wood cell wall, it may be considered that a LCC situated at the interface between polysaccharide and lignin and reinforces the poor interfacial adhesion.

Acknowledgment

The author wishes to express his indebtedness to Prof. Isao Sakata, Kyushu University, for his enthusiastic discussion and helpful suggestion in detail. The author is deeply grateful to Prof. Kokki Sakai, Kyushu University, and Assoc. Prof. Mitsuo Higuchi, Kyushu University, for their valuable suggestions and a critical reading of this manuscript.

Further, the author is grateful to Prof. Gohsuke Sugihara, Fukuoka University, and Dr. Mitsuhiro Morita, Kyushu University, for their kind advice and encouragement.

Great thanks are due to Assoc. Prof. Tohru Inoue, Fukuoka University, for the investigation by differential scanning calorimetric measurement.

Thanks are also due to all members of the Department of Forest Products, Faculty of Agriculture, Kyushu University for their kind help and discussions.

References

[1] A. Frey-Wyssling, *Wood Sci. Technol.*, **2**, 73-83 (1968).
[2] A. J. Kerr, D. A. I. Goring, *Cellul. Chem. Technol.*, **9**, 563-573 (1975).
[3] K. Ruel, F. Barnoud, D. A. I. Goring, *Wood Sci. Technol.*, **12**, 287-291 (1978).
[4] P. Erins, V. Cinite, M. Jakobsons, J. Gravitis, *Appl. Polym. Symp.*, **28**, 1117-1138 (1976).
[5] M. Dambis, M. Jakobsons, J. Gravitis, P. Erins, *Khim. Drev.*, No.1, 14-18 (1981); [*Chem. Abst.*, **94**, 176945].
[6] J. Gravitis, P. Erins, *Appl. Polym. Symp.*, **37**, 421-440 (1983).
[7] J. Gravitis, B. Andersons, M. Jakobsons, I. Dumina, P. Erins, *Khim. Drev.*, No.5, 99-102 (1984); [*Chem. Abst.*, **101**, 212909].
[8] D. R. Paul, S. Newman, Eds., "*Polymer Blends*", Academic, New York 1978, vol.1.
[9] O. Olabishi, L. M. Robeson, M. T. Shaw, "*Polymer-Polymer Miscibility*", Academic, New York 1979.
[10] D. Rigby, J. L. Lin, R. J. Roe, *Macromolecules*, **18**, 2269-2273 (1985).
[11] A. Björkman, *Svensk Papperstidning*, **59**, 477-485 (1956).
[12] A. Björkman, B. Person, *Svensk Papperstidning*, **60**, 158-169 (1957).
[13] A. Björkman, *Svensk Papperstidning*, **60**, 243-251 (1957).
[14] A. Björkman, B. Persson, *Svensk Papperstidning*, **60**, 285-292 (1957).
[15] A. Björkman, *Svensk Papperstidning*, **60**, 329-335 (1957).
[16] S. Takase, N. Shiraishi, M. Takahama, *Abstracts Papers of CELLUCON 88 Japan*, Kyoto, 1988, p.35.: "*Wood Processing and Utilization*", J. F. Kennedy, G. O. Phillips, P. A. Williams, Eds., Ellis Horwood, Southampton 1989, p.243-249.
[17] M. Morita, M. Shigematsu, I. Sakata, *Cellul. Chem. Technol.*, **21**, 255-265 (1987).
[18] M. Morita, T. Koga, M. Shigematsu, I. Sakata, "*Wood Processing and Utilization*", J. F. Kennedy, G. O. Phillips, P. A. Williams, Eds., Ellis Horwood, Southampton 1989, p.293-298
[19] N. Shiraishi, *Kobunshikako*, **38**, 338-344 (1989).
[20] T. G. Rials, W. G. Glasser, *J. Appl. Polym. Sci.*, **37**, 2399-2415 (1989).
[21] T. G. Rials, W. G. Glasser, *Wood and Fiber Sci.*, **21**, 80-90 (1989).
[22] M. Shigematsu, M. Morita, I. Sakata, *Mokuzai Gakkaishi*, **37**, 50-56 (1991).
[23] M. Shigematsu, M. Morita, I. Sakata, *Mokuzai Gakkaishi*, in press.
[24] P. J. Flory, "*Principles of Polymer Chemistry*", Cornell University Press, Ithaca 1953, Chapter 12.
[25] M. Shigematsu, M. Morita, I. Sakata, *Makromol. Chem.*, in press.
[26] E. Hägglund, B. Lindberg, J. McPherson, *Acta Chem. Scand.*, **10**, 1160-1164 (1956).
[27] H. O. Bouveng, P. J. Garegg, B. Lindberg, *Acta Chem. Scand.*, **14**, 742-748 (1960).
[28] L. E. Wise, M. Murphy, A. A. D'Addieco, *Paper Trade J.*, **122**(2), 35 (1946).
[29] B. L. Browning, "*Methods of Wood Chemistry,* vol.II", John Wiley & Sons, New York 1967, p.732.
[30] T. Koshijima, T. Taniguchi, R. Tanaka, *Holzforschung*, 26, 211-217 (1972).
[31] TAPPI Standard T 13 m-54.
[32] B. Lindberg, K. Rosell, S. Svensson, *Svensk Papperstidning*, **76**, 30-32 (1973).
[33] D. Fengel, G. Wegener, "*Wood: Chemistry, Ultrastructure, Reactions*",

Walter de Gruyter, Berlin 1984, p.106.
[34] R. H. Marchessault, C. Y. Liang, *J. Polym. Sci.*, **59**, 357-378 (1962).
[35] R. H. Marchessault, W. Settineri, W. Winter, *Tappi*, **50**(2), 55-59 (1967).
[36] D. A. I. Goring, "*Lignins*", K. V. Sarkanen and C. H. Ludwing, Eds., Wiley Interscience, New York 1971, Chapter 17.
[37] R. G. LeBel, D. A. I. Goring, *J. Polym. Sci. Part C*, **2**, 29-48 (1963).
[38] A. Razanowich, W. Q. Yean, D. A. I. Goring, *Svensk Papperstidning*, **66**, 141-149 (1963).
[39] M. V. Ramiah, D. A. I. Goring, *J. Polym. Sci. Part C*, **11**, 27-48 (1965).
[40] B. Košíková, L. Zákutná, D. Joniak, *Holzforschung*, **32**, 15-18 (1978).
[41] H. H. Brownell, *Tappi*, **53**(7), 1278-1281 (1970).
[42] F. Yaku, S. Tsuji, T. Koshijima, *Holzforschung*, **33**, 54-59 (1979).
[43] F. Yaku, R. Tanaka, T. Koshijima, *Holzforschung*, **35**, 177-181 (1981).
[44] A. N. Gent, G. R. Hamed, "*Encyclopedia of Polymer Science and Engineering, 2nd Edition*", H. F. Mark, N. M. Bikales, C. G. Overberger, G. Menges, Eds., John Wiley & Sons, New York 1985, vol.1, p.476-518.
[45] P. R. Gupta, A. Rezanowich, D. A. I. Goring, *Pulp Paper Mag. Can.*, T21-27 (1962).
[46] T. D. Pendle, "*Block and Graft Copolymerization*", R. J. Ceresa, Ed., Wiley, New York 1973, vol.1, p.83.
[47] J. W. Schurer, A. de Boer, G. Challa, *Polymer*, **16**, 201 (1975).
[48] D. R. Paul, "*Polymer Blends*", D. R. Paul, S. Newman, Eds., Academic, New York 1978, vol.1, Chapter 12.
[49] H. Inoue, A. Matsumoto, K. Matsukawa, A. Ueda, S. Nagai, *J. Appl. Polym. Sci.*, **41**, 1815-1829 (1990).
[50] T. K. Kwei, T. T. Wang, "*Polymer Blends*", D. R. Paul, S. Newman, Eds., Academic, New York, 1978, vol. 1, Chapter 4.
[51] O. Olabisi, L. M. Robeson, M. T. Shaw, "*Polymer-Polymer Miscibility*", Academic, New York 1979, Chapter 2
[52] Koubunshi Gakkai, Ed., "*Polymer Alloy*", Tokyo Kagaku Dojin 1981.
[53] S. Akiyama, *Kobunshi*, **29**, 819-822 (1980).
[54] M. Bank, J. Leffingwell, C. Thies, *J. Polym. Sci. Part A-2*, **10**, 1097-1109 (1972).
[55] T. Inoue, H. Saito, *Kobunshi*, **38**, 288-291 (1989).
[56] R. Roe, "*Encyclopedia of Polymer Science and Engineering, 2nd Edition*", H. F. Mark, N. M. Bikales, C. G. Overberger, G. Menges, Eds, John Wiley & Sons, New York, 1985, vol.7, p.531-544.
[57] J. J. Aklonis, W. J. MacNight, M. Shen, "*Introduction to Polymer Viscoelasticity*", Wiley-Interscience, New York 1972.
[58] D. W. van Krevelen, "*Properties of Polymers - Correlations with Chemical Structure*", Elsevier, Amsterdam 1972.
[59] E. L. Back, N. L. Salmen, *Tappi*, **65**(7), 107 (1977).
[60] N. L. Salmen, E. L. Back, *Tappi*, **65**(12), 137 (1977).
[61] D. A. I. Goring, *Pulp Paper Mag. Can.*, **64**, T512-527 (1963).
[62] G. M. Irvine, *Tappi J.*, **67**(5), 118-121 (1984)
[63] M. Tanahashi, T. Aoki, T. Higuchi, *Mokuzai Gakkaishi*, 27, 116-124 (1981).
[64] D. R. Paul, J. W. Barlow, H. Keskkula, "*Encyclopedia of Polymer Science and Engineering, 2nd Edition*", H. F. Mark, N. M. Bikales, C. G. Overberger, G. Menges, Eds, John Wiley & Sons, New York 1985, vol.12, p.399-461.
[65] W. N. Kim, C. M. Burns, *J. Polym. Sci. Part B*, **28**, 1409-1429 (1990).
[66] W. N. Kim, C. M. Burns, *J. Appl. Polym. Sci.*, **41**, 1575-1593 (1990).
[67] L. A. Wood, *J. Polym. Sci.*, **28**, 319 (1958).

[68] T. G. Fox, *Bull. Am. Phys. Soc.*, **1**(2), 123 (1956).
[69] P. R. Couchman, *Macromolecules*, **11**, 1156 (1978).
[70] R. L. Scott, *J. Chem. Phys.*, **17**, 279 (1949).
[71] H. Tompa, *Trans. Faraday Soc.*, **45**, 1142 (1949).
[72] B. Košíková, D. Joniak, M. Košík, *Cellulose Chem. Technol.*, **9**, 61-70 (1975)
[73] I. N. Levine, "*Physical Chemistry*", McGraw-Hill Kogakusha, Tokyo 1978, p.298.
[74] D. Rigby, J. L. Lin, R. J. Roe, *Macromolecules*, **18**, 2269-2273 (1985).
[75] T. Nishi, *J. Macromol. Sci. Phys. Ed.*, **B17**, 517-542 (1980).
[76] R. J. Roe, W. C. Zin, *Macromolecules*, **13**, 1221 (1980).
[77] T. Shiomi, K. Kohno, K. Yoneda, T. Tomita, M. Miya, K. Imai, *Macromolecules*, **18**, 414-419 (1985).
[78] M. Shibayama, H. Yang, R. S. Stein, C. C. Han, *Macromolecules*, **18**, 2179-2187 (1985).
[79] C. Schuerch, *J. Am. Chem. Soc.*, **74**, 5061-5067 (1952).
[80] W. Brown, *J. Appl. Polym. Sci.*, **11**, 2381-2396 (1967).
[81] M. Remko, J. Polčin, *Z. Phys. Chem. Neue Folge*, **126**, 195-204 (1981).
[82] S. Wu, "*Polymer Blends*", D. R. Paul, S. Newman, Eds, Academic, New York 1978, vol.1, Chapter 6.
[83] A. K. Rastigi, L. E. ST. Pierre, *J. Colloid & Interface Sci.*, **31**, 168-175 (1969).
[84] F. M. Fowkes, "*Advances in Chemistry Series 43: Contact Angle, Wettability, and Adhesion*", R. F. Gould, Ed., American Chemical Society, Washington 1964, p.99-111.
[85] R. E. Johnson, R. H. Dettre, "*Surface and Colloid Science*", vol.2, E. Matijević, Ed., Wiley-Interscience, New York 1969, p.85-153
[86] J. A. Riddick, W. B. Bunger, T. K. Sakano, Eds., "*Organic Solvents: Physical Properties and Methods of Purification*", Fourth Edition, John Wiley & Sons, New York 1986.
[87] T. Hata, *Kobunshi*, **17**, 564-605 (1968).
[88] F. M. Fowkes, "*Treatise on Adhesion and Adhesives*", R. L. Patrick, Ed., Marcel Dekker, New York 1967, vol.1, Chapter 9.
[89] T. Young, *Phil. Trans. Roy. Soc. (London)*, **95**, 65 (1805).
[90] H. W. Fox, W. A. Zisman, *J. Colloid Sci.*, **5**, 514 (1950).
[91] W. A. Zisman, "*Advances in Chemistry Series 43: Contact Angle, Wettability, and Adhesion*", R. F. Gould, Ed., American Chemical Society, Washington 1964, p.1-51.
[92] P. Luner, M. Sandell, *J. Polym. Sci. Part C*, **28**, 115-142 (1969).
[93] S. B. Lee, P. Luner, *Tappi*, **55**(1), 116-121 (1972).
[94] J. R. Dann, *J. Colloid & Interface Sci.*, **32**, 302, 321 (1970).
[95] L. A. Girifalco, R. J. Good, *J. Phys. Chem.*, **61**, 904-909 (1957).
[96] Y. Kitazaki, T. Hata, *Nihon-setchaku-kyokaishi*, **8**, 131-142 (1972).
[97] D. K. Owens, R. C. Wendt, *J. Appl. Polym. Sci.*, **13**, 1711-1717 (1969).
[98] B. R. Ray, J. R. Anderson, J. J. Scholz, *J. Phys. Chem.*, **62**, 1220 (1958).
[99] J. L. Rosano, *Mem. Serv. Chim. Etat (Paris)*, **36**, 437 (1951).
[100] C. G. L. Furmidge, *J. Colloid Sci.*, **17**, 309 (1962).
[101] D. C. Pease, *J. Phys. Chem.*, **49**, 107 (1945).
[102] W. D. Bascom, *Adv. Polym. Sci.*, **85**, 90 (1988).
[103] A. Takahara, N-J. Jo, T. Kajiyama, *J. Biomater. Sci. Polym. Edit.*, 1, 29 (1989).

Nomenclature

Symbol	Description	Typical unit
(Chapter 1)		
C	: spreading concentration of lignin in cellulose/lignin system	mg/cm^2
C_{LCC}	: spreading concentration of LCC in multilayer system	$\mu g/cm^2$
$C_{LCC.max}$	: C_{LCC} giving the maximum of σ	$\mu g/cm^2$
f_2	: mass fraction of lignin in LCC molecules	
σ	: interlaminar bond strength	kgf/cm^2
(Chapter 2)		
B	: interaction energy for mixing segments ($B=\Delta V_r=RT\chi$)	J
f_1	: mass fraction of polysaccharide in LCC molecules	
f_2	: mass fraction of lignin in LCC molecules ($f_1+f_2=1$)	
g_0	: composition independent term of χ_{12}	
g_1	: composition dependent term of χ_{12}	
g_{0A}	: composition independent and temperature independent term of χ_{12}	
g_{1A}	: composition dependent and temperature independent term of χ_{12}	
g_{0B}	: composition independent and temperature dependent term of χ_{12}	
g_{1B}	: composition dependent and temperature dependent term of χ_{12}	
$\bar{M}_n$	: number average molecular weight	g/mol
$\bar{M}_v$	: viscosity average molecular weight	g/mol
R	: gas constant	J/K·mol
T	: absolute temperature	K
T_b	: binodal temperature of ternary-blends system	K
$T_{b.0}$	: binodal temperature of binary-blends system	K
Tg	: glass transition temperature	K
V_i	: molar volume of i-th polymer	cm^3/mol
V_r	: reference volume, usually taken to the molar volume of a segment	cm^3
ΔG_M	: free energy of mixing	J/mol
ΔH_M	: enthalpy of mixing	J/mol
ΔS_M	: entropy of mixing	J/K·mol
ϕ_1	: volume fraction of hemicellulose in the blend	
ϕ_2	: volume fraction of lignin in the blend	
ϕ_3	: volume fraction of LCC in the blend ($\phi_1+\phi_2+\phi_3=1$)	
ϕ_L	: overall volume fraction of lignin in ternary-blends system ($\phi_L=\phi_2+f_2\phi_3$)	
Λ	: interaction energy density	J/cm^3
λ_0	: temperature independent term of Λ	J/cm^3
λ_T	: temperature dependent term of Λ	$J/cm^3 \cdot K$
ρ	: density	g/cm^3
ξ	: volume fraction of lignin into homopolymers in ternary-blends system ($\xi=\phi_2/(\phi_1+\phi_2)$)	
χ_{12}	: Flory polymer-polymer interaction parameter between hemicellulose and lignin	

Symbol	Description	Typical unit
(Chapter 3)		
a_o	: activity of solvent in solution	
C	: concentration of solution	g/g
K_1	: calibration constant based on molality	g/mol·Ω
K_2	: calibration constant based on mol fraction	mol/mol·Ω
$\bar{M}_n$	: number average molecular weight	g/mol
$\bar{M}_v$	: viscosity average molecular weight	g/mol
$\bar{M}_w$	: weight average molecular weight	g/mol
R	: gas constant	J/K·mol
T	: absolute temperature	K
v_o	: volume fraction of solvent (DMSO) in solution	
v_1	: volume fraction of hemicellulose in solution	
v_2	: volume fraction of lignin in solution	
V_o	: molar volume of solvent (DMSO)	cm^3/mol
$\Delta\bar{G}_o$	: free energy of dilution	J/mol
$\Delta\bar{H}_o$	: enthalpy of dilution	J/mol
ΔR	: resistance difference of the two thermistors in vapor pressure osmometer	Ω
$\Delta\bar{S}_o$	: entropy of dilution	J/K·mol
δ	: solubility parameter	$(cal/cm^3)^{1/2}$
Λ	: interaction energy density	J/cm^3
$[\eta]$	: intrinsic viscosity	dl/g
ρ	: density	g/cm^3
ξ	: volume fraction of lignin into polymers in ternary solution ($\xi=v_2/(v_1+v_2)$)	
χ	: Flory polymer-polymer interaction parameter	
χ_{o1}	: χ between DMSO and hemicellulose	
χ_{o2}	: χ between DMSO and lignin	
χ_{12}	: χ between hemicellulose and lignin	
χ^*	: χ between DMSO and existing polymers	
(Chapter 4)		
α	: tilted plane angle	degree
π_e	: spreading pressure of vapor on solid surface	dyne/cm
θ	: contact angle	degree
θ_a	: advancing contact angle	degree
θ_r	: receding contact angle	degree
θ_A	: maximum θ_a by tilting	degree
θ_R	: maximum θ_r by tilting	degree
γ	: surface tension	dyne/cm
γ_C	: critical surface tension	dyne/cm
γ_L	: surface tension of liquid	dyne/cm
γ_S	: surface tension of solid	dyne/cm
γ^d	: dispersion force contribution to γ	dyne/cm
γ^p	: polar force contribution to γ	dyne/cm
γ_{LV}	: liquid-vapor surface tension	dyne/cm
γ_{SL}	: solid-liquid surface tension	dyne/cm
γ_{SV}	: solid-vapor surface tension	dyne/cm

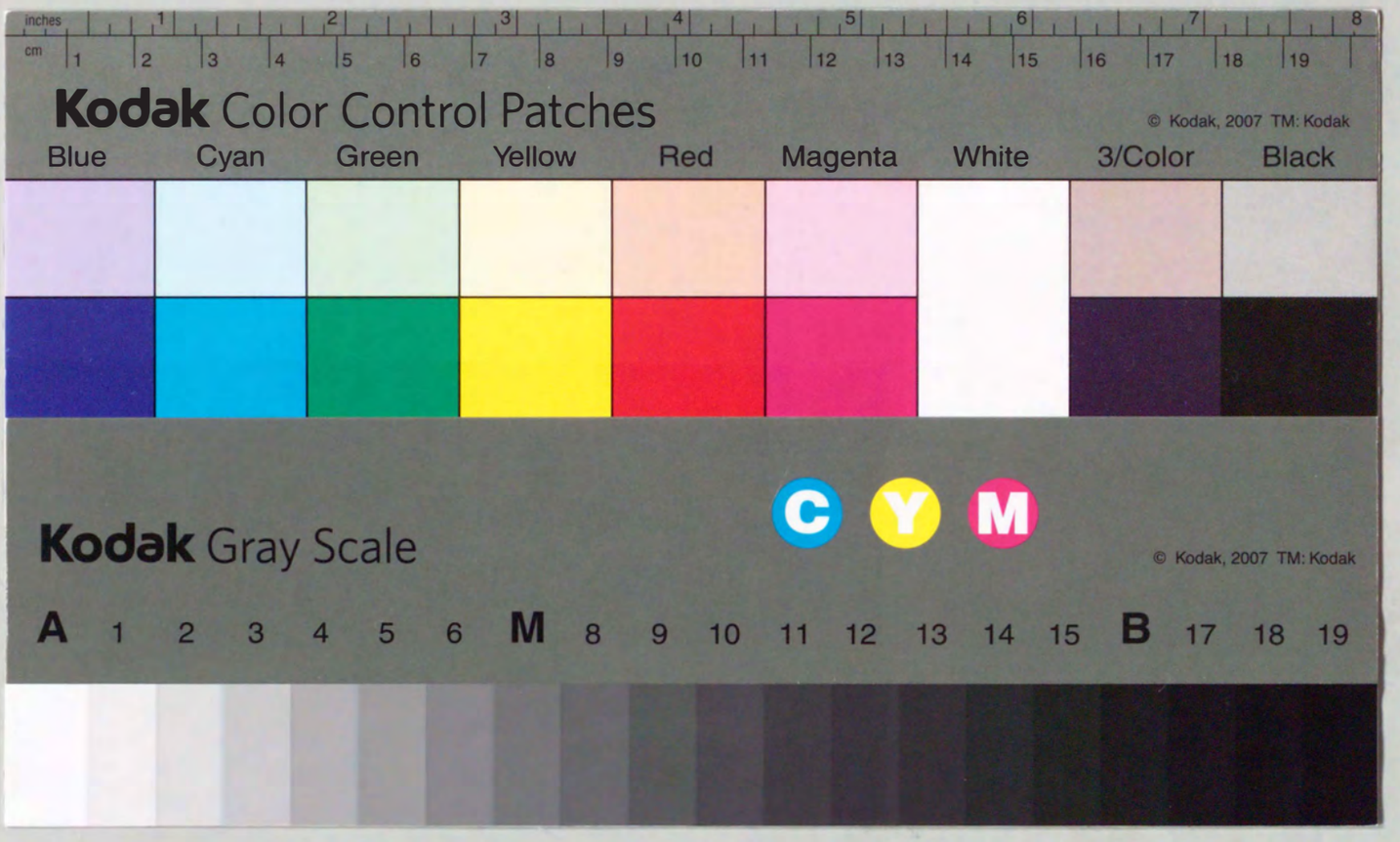
inches
cm
Kodak Color Control Patches
© Kodak, 2007 TM: Kodak
Blue
Cyan
Green
Yellow
Red
Magenta
White
3/Color
Black
Kodak Gray Scale
C
Y
M
© Kodak, 2007 TM: Kodak
A 1 2 3 4 5 6 M 8 9 10 11 12 13 14 15 B 17 18 19